Role of tides in Arabian Gulf circulation and long-term exchange with the Sea of Oman

M Salim[1], Maryam R. Al-Shehhi[1*], Hajoon Song[2] and Jean-Michel Campin[3], Chris Hill[3], and John Marshall[3]

[1]Khalifa University, Civil and Environmental Engineering, Abu Dhabi, United Arab Emirates,
[2]Yonsei University, Department of Atmospheric Sciences, Seoul, South Korea.
[3]Massachusetts Institute of Technology, Cambridge, MA, United States

Corresponding author: (maryamr.alshehhi@ku.ac.ae)

Phone Number: +97128109188

Abstract

The Arabian Gulf is a semi-enclosed marginal sea located along the northern boundary of the Arabian Peninsula. The tides and its role in the circulation of the Gulf are still uncertain and most previous modeling studies have neglected them. Here, we explore the tide-induced residual circulation in the Gulf using a high resolution 3-dimensional model based on the MITgcm, including high resolution bathymetry and a representation of the tidal currents of seven major constituents (M2, S2, N2, K2, K1, O1, and P1) which are prescribed at the open boundaries. The simulation shows good agreement with observed tidal elevations and tidal-scale currents across the interior of the Gulf. Tide-induced residual currents are found to be significant in the Strait of Hormuz where they cause major rectification of current speeds and patterns in the Strait and also in shallow, high-slope bathymetry regions of the inner Gulf. We find that tides result in strong enhancement of vertical mixing, especially towards the center of the Gulf during winter with weak enhancement during the summer. The summer and winter analysis of transport shows that tidal action causes a greater rectification in summer than in winter. The asymmetry in tidal action on inflow compared to outflow results in a roughly 30% enhancement of net inflow through the Strait of Hormuz. We conclude that tides strongly influence the volume exchange between the Gulf and the Sea of Oman through the Strait and must be included in ocean models that attempt to represent the general circulation.

1. Introduction

The Arabian Gulf is a shallow, semi-enclosed marginal sea located along the northern boundary of the Arabian Peninsula (Figure 1). The Arabian Gulf is connected to the Sea of Oman through the Strait of Hormuz. The Gulf is in an arid region with excess of evaporation affecting ocean circulation and exchange with the Sea of Oman and Arabian Sea (Johns et al., 2003; Kämpf and Sadrinasab, 2006; Pous et al., 2015). The region is also affected by the *Shamal* winds, which blow northwesterly throughout the year along the axis of the Gulf (Abdelrahman and Ahmad, 1995). The general circulation in the Gulf is dominated by a cyclonic barotropic gyre between spring and summer which breaks in to smaller features as the wind intensifies (Kämpf and Sadrinasab, 2006; Pous et al., 2015).

Circulation and transport in the Gulf are also affected by tides. Tides can enhance inflow and outflow and contribute to the net long-term exchange through the Strait (Farmer and Armi, 1986; Naranjo et al., 2014; Sannino et al., 2015, 2004). In early studies, low resolution two dimensional tidal models focused on simulating tidal constituents and phases (Bashir et al., 1989; Lardner et al., 1986, 1982; Von Trepka, 1968). Although these models helped in describing the structure of tidal constituents, the results were not in a close agreement with tidal charts due to the neglect of non-linear interaction and the use of a coarse grids. Later studies applied three dimensional models at higher resolution (Lardner et al., 1989; Lardner and Cekirge, 1988) and included more tidal constituents (Proctor et al., 1992). These improved the estimation of tides in the Gulf, enabling them to be mapped, including the identification of amphidromic points. In addition observational studies have analyzed basin-wide moored tidal current measurements (John, 1992) and direct observations collected during the Mt. Mitchell expedition (Reynolds, 1993). These revealed that:

tides in the Gulf are complex varying from semi-diurnal to diurnal motions; barotropic tidal currents in the Strait of Hormuz are dominant and significant throughout the water column and exhibit a large asymmetry between flood and ebb tides; the peak value of the M2 tidal current in the Strait of Hormuz is order 2 ms^{-1}; the semi-diurnal and diurnal constituents generate a resonant oscillation with amphidromic points, two associated with the semi-diurnal tidal constituents (M2 and S2) in the south-west and south-east of the Gulf and one associated with diurnal constituents (K1 and O1) in the central southern Arabian Gulf (nearby Bahrain).

Several studies have included tides in general circulation models to capture the combined effects of tides and wind-driven circulation. For example, Al-Rabeh et al. (1990) and Kämpf and Sadrinasab (2006) prescribed tidal amplitudes at the Strait of Hormuz in a three-dimensional model. Sabbagh-Yazdi et al. (2007) estimated tidal currents and both Chu et al. (1988) and Vasou et al. (2020) have included tides in their models to study circulation and exchange through the Strait. Alosairi et al. (2011), Hughes and Hunter (1979) and Pous et al. (2012) find that tides dominate instantaneous flow fields but play a negligible role in setting the time-mean general circulation. For example. Pous et al. (2012) used a barotropic tidal model and noted tidal currents exceeding 1 m s^{-1} in the Strait of Hormuz but with a weak net circulation of order 2 cm s^{-1}. In contrast, Alosairi et al. (2011) show that tides can generate large lateral shears and are responsible for stronger currents in the Gulf. Mashayekh Poul et al. (2016b) applied a barotropic model to a study of the impact of subsea bed salt domes on residual tides, and found strong tide-induced residual currents. They observed residual currents induced by the M2 tide of order 15 cm s^{-1}, more than 5 times greater than previous studies.

The above conflicting results suggest that there is a need for a more comprehensive study of the role of tides and their importance, or otherwise, in setting the residual flow of the Gulf. In this study, therefore, we implement a very high resolution baroclinic model of the Gulf and its connection to the Sea of Oman, and use it to: (i) model the diurnal and semi-diurnal tides within the Gulf and compare with observations, (ii) characterize the tidal residual circulation in the Gulf, (iii) estimate the net transport through the Strait of Hormuz, and (iv) evaluate the effect of tidal forcing on the exchange and mixing over different seasons.

Our paper is organized as follows. Section 2 contains a description of the model used to simulate tides in the Gulf. In section 3, model results are compared with available data of surface elevation and currents. Section 4 includes the description of the tidal features in the Gulf. Section 5 explores the tidal effect on the general circulation including mixing and transport through the Strait of Hormuz, while summary and conclusions complete the paper.

2. Modeling framework and approach

We deploy a high resolution version of the Massachusetts Institute of Technology general circulation model (MITgcm) (Marshall et al., 1997), that has been extensively used in studies of tides, internal tides and residual currents in coastal waters in the presence of complex topographies and geometries (Sannino et al., 2015; Wang et al., 2015). The model is configured for the Arabian Gulf and Sea of Oman (23.2^{o}N to 30.7^{o}N and 47.3^{o}E to 62.3^{o}E) as shown in Figure 1. It has a high horizontal spatial resolution of approximately 2.5 km and 83 vertical levels ranging from 1 m resolution at the surface to ~200 m at the bottom out in the Sea of Oman. A high resolution bathymetry data set derived in Smith and Sandwell (1997) is used in the model with a resolution

of 3 km. The initial temperature and salinity is obtained from a 1/48 degree MITgcm global model simulations called LLC4320 (Rocha et al., 2016) and the data is extracted for the coastal areas of Arabian Gulf and Sea of Oman. A horizontal viscosity of 10 $m^2 s^{-1}$, a vertical viscosity of $1x10^{-4}$ $m^2 s^{-1}$, and bottom drag coefficient of 2.5×10^{-3} $m^2 s^{-1}$ is specified through the domain uniformly. A standard configuration of the nonlocal K-profile parameterization (KPP) (Large et al., 1997, 1994) is used to parameterize ocean turbulent mixing and thereby determine the depth of the ocean surface boundary layer with a background vertical diffusivity of 5.4×10^{-7} m^2 s^{-1}.

To study the effect of tides on the general circulation within the Gulf, we designed three numerical experiments driven by: (i) tides only; (ii) atmospheric forcing with no tides, and (iii) both tides and atmospheric forcing. The meteorological forcing data is obtained from an ECMWF operational dataset at a resolution of 6-hours. The tidal constituents (M2, S2, N2, K1, O1, and P1) are taken from the Arabian Sea regional barotropic tidal model (OTIS) (Egbert et al., 1994; Egbert and Erofeeva, 2002). In the tide-only run, we have taken the approach of Alisairi et al (2011), in which the diffusion of temperature and salinity is not represented by setting the horizontal and vertical diffusivities to zero. In all three scenarios, the model was run for 7 years with repeating surface forcing and boundary conditions, and the first 6 years considered as the spin-up period.

The simulated instantaneous current (u) includes three terms, a steady residual current (u_a), a perturbation current (u_ε) and the tidal current ($u_{bi} \cos(\omega t+\varphi_i)$), where ω_i and φ_i are the frequency and phase for the seven (i) tidal constituents. The tidal current is computed following the approach described in Foreman (1978) by identifying the tidal semi-diurnal components M2, S2, N2, K2 and the diurnal components K1, O1 and P1 of the u and v currents. After obtaining the tidal current

comprising these seven tidal components, it is removed from the instantaneous current following the procedure described in Nayak et al. (2015) to arrive at the resultant current ($u_a + u_\varepsilon$). This is then averaged over multiple tidal cycles to remove the perturbation component to yield the steady residual current (u_0).

3. Evaluation of modeled tides against tide-gauge observations

The tidal components retrieved from MITgcm are compared with in-situ observations in Sections 3.1 and 3.2 to examine model performance with a focus on tidal constituents and residual circulation.

3.1 Tidal constituents

Our model performance is evaluated through comparison with major tidal constituents (M2, S2, K1 and O1) at 37 tide gauge stations distributed over the Gulf and Sea of Oman. The tide gauge data are obtained from the International Hydrographic office and published by Pous et al. (2012). Figure 2 shows M2, S2, K1 and O1 extracted from MITgcm versus the observed data. Close agreement between the model and observed tidal elevations and phases of M2, S2, K1 and O1 is found. The corresponding correlation (R^2) values between modeled and observed tidal amplitudes are encouraging with values of 0.82, 0.84, 0.62, and 0.80, respectively. Similarly, high R^2 values are found between the modelled and observed tidal phases (0.92, 0.91, 0.93 and 0.96), at M2, S2, K1 and O1. In addition, the model is able to reproduce the amphidromic points caused by the diurnal and semi-diurnal tidal constituents (Figure 3).

To further quantitatively assess predicted tidal amplitudes, the root mean square error (RMSE) for each tidal constituent at each coastal tide-gauge station is estimated as follows:

$$RMSE = \sqrt{\frac{1}{T}(A_o \cos(\omega t - \varphi_o) - A_m \cos(\omega t - \varphi_m))^2} \ ,$$

where A and φ are the complex amplitude and phase respectively obtained from observed and modelled tidal levels and T is the length of the time sample. The model shows good agreement with the observations in both the Arabian Gulf and Sea of Oman. The average RMSE values for tidal levels at M2, S2, K1 and O1 are 13.5, 8.08, 6 and 4.8 cm, respectively. The RMSE of M2 is a maximum of 15 cm or so at the 4 stations near Qatar and Bahrain where the water is very shallow. However, elsewhere in the Gulf, the RMSE does not exceed 10 cm.

3.2 Tidal-scale currents

Instantaneous ocean currents *u* and *v* are compared with time series data obtained from five mooring stations (Reynolds, 1993) at different depths (10m, 15 m, 21 m, 24 m, 30 m, 40 m, 56 m and 84 m). The skill of the model is measured using Willmott's method (Willmott, 1981) as described by Warner et al., (2005). Skill values vary from 0, indicating complete disagreement, to 1, perfect agreement, between model and observation thus:

$$skill = 1 - \frac{\sum_{i=1}^{n} |Y_{model} - Y_{observed}|^2}{\sum_{i=1}^{n} (|Y_{model} - \overline{Y_{observed}}| + |Y_{observed} - \overline{Y_{observed}}|)^2} \ .$$

Our model reproduces the currents with an average model skill value of 0.7 for both *u* and *v* However, the lowest skill values of 0.5-0.6 for the *v* component are found at mooring M2. The tidal current analysis at M2 shows that it is dominated by tidal currents. The maximum modeled *u* and *v* values of the 10 m current are 22.7 cm s^{-1} and 6 cm s^{-1}, respectively, in good agreement with the observations (22.6 cm s^{-1} and 6.49 cm s^{-1}). The magnitudes of the currents decrease with depth. For example, at 40 m the modelled *u* and *v* components at M2 are 14 and 10.1 cm s^{-1}, respectively,

which are close to the observed values of 13 and 8.6 cm s^{-1}. The time series plot of observed currents at each mooring location is shown in the Appendix (Figure A1 and Figure A2).

4. Tidal Features

Given that our model successfully captures tidal constituents and instantaneous currents at mooring locations, as described in section 3, we now use it to explore the spatial pattern of tidal features in the Gulf region.

4.1 Tides in the Gulf

The spatial distribution of the amplitudes and phases of modeled tidal components M2, S2, K1 and O1 are shown in Figure 3. As can be seen, the most notable tidal feature are: (i) highest amplitudes of M2, S2 and K1 in the Strait of Hormuz, and (ii) the presence of mixed semi-diurnal and diurnal tides in the Gulf. There are two amphidromic points caused by the semi-diurnal tides: one in the south-eastern region of the Gulf near the coast of Abu Dhabi and the other in the south-western side of the Gulf. In contrast, there is an amphidromic point caused by diurnal tides in the south-central region of the Gulf off the coast of Bahrain. Based on these patterns, the M2 tide is the most dominant constituent throughout the Gulf and Sea of Oman, followed by K1, S2 and O1. The M2 tide reaches a maximum amplitude of 149 cm in strongly shoaling and narrowing regions such as the north-western end of the Gulf and near the Iranian coastal region off the Strait of Hormuz. Similarly, K1 dominates over S2 in most of the Gulf, except the areas surrounding the Strait of Hormuz and the diurnal amphidromic point. A maximum K1 amplitude of 48 cm is observed on the western coast of UAE (Abu Dhabi) near Qatar and on the eastern side of the UAE adjacent to the Omani coastal area of the Sea of Oman. The S2 tide reaches a maximum value of 68 cm on the Iranian coast off Hormuz strait. The diurnal component O1 follows the pattern of K1 but has a maximum value of 27 cm.

4.2 Flood and Ebb of Tidal Currents

Tidal currents in the Gulf are described here in respect of flood and ebb conditions. These refer to the tidal phase during rising and falling water levels, respectively. During the flood condition, water flows into the Gulf from the Sea of Oman as shown in Figure 4. Flow speeds reach a maximum of 2.3 m s^{-1} in the Strait of Hormuz flowing in a south-west direction. This current continues to flow into the Gulf parallel to the Iranian coast and merges with the incoming flow from the north-west at the periphery of Kish Island before being redirected towards the Abu Dhabi coast. There are also strong currents flowing south-west along the coasts of UAE (from Ras Al Khaimah to Abu Dhabi) and south-east parallel to the coast of Qatar towards Abu Dhabi. The direction of the flow is significantly affected by the semi-diurnal amphidromic point. For example, currents are directed away from the northern semi-diurnal amphidromic toward the south-east and north-west. In addition, the current on the western side of the Gulf is pulled south-east towards the low-lying semi-diurnal amphidromic point near Abu Dhabi Coast. This phenomenon causes a strong net tidal current near Abu Dhabi with a maximum speed of 2.1 m s^{-1} but weak tidal currents near Hendorabi Island across the Gulf along the coast of Iran.

In contrast, during ebb conditions, the water is flushed out from the Gulf. As shown in Figure 4, there is a strong ebb flow at the Strait of Hormuz towards the northeast which then turns south-east towards the Sea of Oman. Similarly, a strong tidal current is observed around the north and eastern coastlines of Qatar during the ebb phase, which is also observed during the flood phase but flowing in the opposite direction. However, there is a relatively weak flow heading north-west towards the diurnal amphidromic point located off the coast of Qatar.

5. The influence of Tides on the general circulation of the Gulf

We now use our model to study the effect of tides on the time-averaged residual circulation, focusing on the long-term exchange and levels of mixing in the Gulf which, as described in the introduction, remain uncertain.

5.1 Tide-induced residual circulation in the Gulf

We obtained the tidal residual circulations by removing the chosen frequencies as described in Section 2 and then computing a long-time average. The resultant tidal residual circulations are presented in Figure 5 from our run in which only tidal forcing was present. The tide-induced residual currents show an anticlockwise pattern inside the Gulf steered by bathymetric slope. The interaction of tides with bathymetry drives a significant anti-cyclonic pattern in the Gulf. We see that residual currents are dominant in areas of sharply changing bathymetry and large slope. In addition, the intensity of the tide-induced residual speeds vary markedly from a few cm s^{-1} to more than 15 cm s^{-1}. The current is strong in the Strait of Hormuz which flows along its central axis toward the north-west parallel to the Iranian coast and extends up to the north of Bahrain. In addition, strong cyclonic tidal residual eddies are seen to the west of the Strait of Hormuz (north of Abu Musa island) driving circulation in the northern region along the Iranian coast. Similarly, to the south, strong currents are observed along the southern coastal boundary near Abu Dhabi islands and at the western boundary of the Gulf. A pair of strong cyclonic and anti-cyclonic eddies are observed surrounding Dalma and Arzana Islands near Abu Dhabi together with an intense flow towards North West exceeding 10 cm s^{-1} in between these Islands. A south-eastward flowing current is also found flowing parallel to the coast of Qatar. At the center of the Gulf, two main cyclonic patterns of residual currents are observed between Qatar and Iran. Such eddies have been also observed by (Mashayekh Poul et al., 2016a) in their high resolution barotropic model. These

patterns of tide-induced residual currents are complicated and influenced by coastline and bathymetry. It is clear that tides could contribute significantly to the mean circulations and long-term exchange, between the Sea of Oman and the Gulf.

5.2. The Role of Tides in Modulating Arabian Gulf's General Circulation

The residual circulation described in section 5.1 suggests that tides have a significant role in the circulation in the Gulf. They are a consequence of oscillatory tidal rectification found over complex topography inducing mixing and nonlinearities. To quantify the effect of tides on the circulations, two experiments are carried out: 1) both tidal and atmospheric forcing is present and 2) only atmospheric forcing is present but without tidal forcing. These are diagnosed over the winter and summer seasons (DJF: December-January-February, JJA: Jun-July-August).

The seasonal average of barotropic current speeds during winter (DJF) and summer (JJA) are shown in Figure 6. The left column plots speeds in the tidal run and the right column is the absolute difference between the tidal and non-tidal run. With tides, current speeds in the winter are weaker than in the summer. The weak winter currents are attributed to the reduced density gradient between the Sea of Oman and the Arabian Gulf resulting from winter cooling effects. In winter the air temperature is lowest, the wind speed is maximum and dry air is brought from the continent over the ocean resulting in higher evaporation than in the summer (Swift and Bower, 2003; Thoppil and Hogan, 2010a). Current speeds change when the tidal component is removed in both seasons. The change is basin-wide along the northern coast of the Gulf, the edges of the deeper channels and the Strait of Hormuz, where the tide-induced residual currents are stronger in both seasons. In the winter, the largest difference between tidal and non-tidal runs is found in the

central Gulf along the northern coasts of the UAE where they reach 6 cms^{-1}. In the summer, tidal effects are largest in the Strait of Hormuz where differences of 8 cms^{-1} or more are found.

In addition to the effect of tides on current speeds, they significantly affect flow patterns. The left and right columns of Figure 7 show the tidal and non-tidal depth-averaged current vectors during winter (DJF) and summer (JJA), respectively. The basin-scale circulation patterns in the tidal run are similar to the patterns found in previous modelling studies (Chao et al., 1992; Thoppil and Hogan, 2010b) and observations (Reynolds, 1993). Based on our calculations, we see that the wind driven current is always directed towards the southeast in both seasons (Abdelrahman and Ahmad, 1995; Thoppil and Hogan, 2010b) because the wind pattern is predominantly north-westerly throughout the year in the Gulf. The north-westward flowing Iranian Coastal Current (ICC), which flows against the wind, is induced by density gradients (Swift and Bower, 2003; Thoppil and Hogan, 2010b). The north-westward flowing ICC penetrates further northward during summer. The more elongated ICC during summer is attributed to the high density gradient between the Gulf and the Sea of Oman owing to evaporation in the summer heat and weaker north-westerly *Shamal* winds (Swift and Bower, 2003; Thoppil and Hogan, 2010b). The south-eastward current from the central Gulf flowing along the north of Qatar towards the UAE coast is found during winter while it is weaker and largely absent in summer.

By comparing the aforementioned circulation patterns in the tidal run (Figure 7: left column) with the non-tidal run (Figure 7: right column), it is noticeable that tides play a lesser role in modifying circulation patterns in summer, when wind and heat flux effects dominate. However, tides

significantly modify the winter circulation patterns. We will see below that this is consistent with the idea that tidally enhanced winter mixing induces circulation changes.

5.3 The role of Tides in mixing

Tides can enhance mixing, a key mechanism in the generation of residual circulation, in addition to the nonlinearities described earlier. We have examined the role of tides by analyzing the summertime and wintertime mixed layer depth (MLD) and diffusivities (provided by the KPP scheme) with and without tides (DiffS). We find that, in both tidal and non-tidal simulations, the MLD is deep during winter, mainly in the center of the Gulf, and very shallow during the summer. Adding tides causes deeper mixing especially in the winter season with a maximum MLD of ~70m in the northern coasts near Kish Island (see Figure 8). The strongest tidal enhancement in winter is ~30 m in the central Gulf. The weakest tidal enhancement is at the Strait of Hormuz with a maximum MLD difference (Tide-no Tide) of 3m (Figures 8-9). This suggest that in the winter the Gulf is vertically well mixed in the model, consistent with observations. Although MLD is shallow during summer and the tidal influence rather small, MLD difference (Tide – no Tide) maps shows a tidal enhancement of less than 15 m in shallow coastal margins (e.g. southern coast). As in their effect on MLD, tides increase diffusivity (DiffS) during winter in the deeper areas and at the Strait of Hormuz (Figures 10-11). However, DiffS is near zero in summer, everywhere except in the coastal margins (Figures 10-11) where tides enhance it.

Based on the MLD and DiffS analysis, we conclude that tidal mixing is in action in the Strait of Hormuz and deeper areas (depth > 15m) when the wind is strongest during winter (Hetzel et al.,

2015). However, during summer, winds are relatively weak (Khonkar, 2009) and Gulf waters are highly stratified preventing mixing except in shallow coastal margins with depths less than 15m.

5.4 The role of tides in the exchange through the Strait of Hormuz

The strong impact of tides on circulation and mixing in the Gulf and Sea of Oman, can significantly affect the exchange through the Strait of Hormuz. Inflow occurs through the shallow northern half of the Strait and outflow through the deeper southern half. Figure 12 shows the vertical cross section (along the line CS shown in Figure 1) of the zonal component of the current vector with and without tidal forcing during summer and winter. Positive values show the eastward outflow (red shading) and the negative values (blue) shows the westward inflow. It is clear that tidal action significantly changes the vertical profile of velocity in the Strait. Tidal action forces the inflow to be confined to the upper north of the CS section and reduces inflow speed. Similarly, tidal action significantly reduces outflow speed in the lower south of CS while enhancing it in the upper south. This leads to a spreading of the outflow throughout the column. It is found that in both summer and winter seasons, there is net flow in the upper 40 m while in the bottom layer there is outflow. Strong surface inflow brings relatively fresh water into the Gulf and outflow carries saltier water into the Sea of Oman. This water-mass eventually sinks into the deeper layers of the Arabian Sea in the form of a gravity current. The summer and winter analysis of transport shows that tidal action causes a reduction of roughly 5% on the inflow and outflow during the winter. In summer, however, the inflow and out-flow speeds are reduced by roughly 25% respectively. The maximum transports by inflow and outflow are found in summer months (exceeding 0.22 Sv) with a minimum in the spring (0.14 Sv).

Such differences hint that the tide will significantly control the net volume transport through the Strait of Hormuz. The addition of barotropic tidal flows induce instabilities which generate baroclinic and internal tides/waves. This enhances vertical mixing and significantly influences inflow and outflow by reducing the speed of the through-flow (Kurogi and Hasumi, 2019; Sannino et al., 2015). The tides are strong enough to reverse the outflow or inflow over the tidal cycle. The large difference in tidal action in the winter compared to the summer indicates that tidal affects are non-linear, the more so when currents are strong. The influence of tides on flow speed is related to the remarkable difference in winter and summer stratification. The water column is highly stratified during the summer season while mixing is enhanced during the winter (Al Azhar et al., 2016; Reynolds, 1993). The viscosity (friction) and the bottom/lateral friction drag result in loss of momentum at inflow/outflow (Kurogi and Hasumi, 2019). The detailed mechanisms behind the role of tidal action on suppressing inflow and outflow needs further investigation.

It is significant that the inclusion of explicit barotropic tidal forcing at the open boundary has a non-negligible effect on the circulation. However, the tidal influence on the spreading of fresher water from the Sea of Oman has been neglected in previous studies, despite the fact that the narrow Strait with steeply changing irregular bathymetry and abruptly changing continental shelf-slope, can induce strongly nonlinear interactions. Figure 13 shows the monthly and seasonal average values of net transport through the Strait of Hormuz during tidal and non-tidal simulations, respectively. The net transport in the tidal run shows a higher value than the non-tidal run in all seasons. The net volume transport is higher in the summer season compared to the winter season and is weak during spring (Feb-April). The highest net volume transport occurs in January (0.017 Sv) and August (0.016 Sv). The net volume transport in April is a slight outflow (0.002 Sv) in the

non-tidal runs, whereas it is reversed to inflow (0.003 Sv) in the tidal run. The strong *Shamal* wind (dry air) during winter causes excessive evaporation (Thoppil and Hogan, 2010a) leading to a net-transport from the Sea of Oman which is highest in January. The tidal run shows a yearly-averaged contribution to net transport of 35%, with highest amplification occurring in the summer when it reaches 50%. As noted above, the tidal influence is slightly stronger on outflow than inflow for both winter and summer. This asymmetry in tidal action causes a relatively higher reduction in outflow speed which in turn enhances the net volume transport through the Strait.

6. Conclusions

The Arabian Gulf is a shallow evaporative basin located in the northwest region of the Indian Ocean. The Gulf is connected to the Sea of Oman to the east through the Strait of Hormuz where tides can affect the inflow and outflow and contribute to the net long-term exchange between the Gulf and the Sea of Oman. The tidal currents in the Gulf are strong relative to that of the general circulation, but the effect of the tidal forces on the latter, are not well known and have often been neglected in past modelling studies. The aim of this paper has been to study the tidal features in the Gulf and evaluate their influence on ocean circulation and long-term exchange through the Strait of Hormuz.

We find that tides can induce residual currents that are significant inside the Gulf and in the Strait of Hormuz. Residual current speeds exceed 0.15 ms^{-1} in some areas as observed by (Mashayekh Poul et al., 2016a). The tidal rectification of the current occurs throughout the Arabian Gulf and Strait of Hormuz. When the model is forced with tides, it results in a major rectification of the current speeds and patterns in the Strait and inner Gulf particularly in areas that are shallow and/or

have extremely sloped bathymetry. The tides in the Strait are strong enough to reverse the outflow or inflow over the tidal cycle. Tides are also found to influence the volume of exchange flow during both summer and winter, but particularly in summer where inflow and outflow amplitudes are reduced by 1/4 or so. The asymmetry in tidal action on inflow and outflow speed causes an enhancement of net exchange by 1/3. The addition of the barotropic tide generates internal waves and enhances vertical mixing, significantly influencing inflow and outflow and reduces the speed of through-flow. The large difference of tidal actions in the winter and summer indicates that the role of tide is non-linear and that tidal amplitudes are seasonal.

In summary, our results indicate that inclusion of an explicit barotropic tidal forcing at the open boundary of regional ocean models of the Gulf has significant effects on the circulation, mixing and the rate of exchange with the open ocean. Finally, the tidal influence on the spreading of fresher water from the Sea of Oman has been overlooked in previous studies, despite the fact that the narrow Strait with irregular bathymetry and abruptly changing continental shelf-slope, might be expected to induce nonlinear interactions. The detailed mechanisms behind the role of tidal action on exchange processes and mixing demands further investigation.

7. Acknowledgements

The authors would like to thank Khalifa University for their generous financial support and Prof. Hosni Ghedira use of his laboratory facilities. H. S. also acknowledges the support by National Research Foundation of Korea (NRF) grant (NRF-2019R1C1C1003663) and Yonsei University.

REFERENCES

Abdelrahman, S.M., Ahmad, F., 1995. A note on the residual currents in the Arabian Gulf. Cont. Shelf Res. 15, 1015–1022. https://doi.org/10.1016/0278-4343(95)80006-Y

Al-Rabeh, A.H., Gunay, N., Cekirge, H.M., 1990. A hydrodynamic model for wind-driven and tidal circulation in the Arabian Gulf. Appl. Math. Model. 14, 410–419. https://doi.org/10.1016/0307-904X(90)90096-N

Al Azhar, M., Temimi, M., Zhao, J., Ghedira, H., 2016. Modeling of circulation in the Arabian Gulf and the Sea of Oman: Skill assessment and seasonal thermohaline structure. J. Geophys. Res. Ocean. 121, 1700–1720. https://doi.org/10.1002/2015JC011038

Alosairi, Y., Imberger, J., Falconer, R.A., 2011. Mixing and flushing in the Persian Gulf (Arabian Gulf). J. Geophys. Res. Ocean. 116, 1–14. https://doi.org/10.1029/2010JC006769

Bashir, M., Khaliq, A.Q.M., Al-Hawaj, A.Y., Twizell, E.H., 1989. An explicit finite difference, model for tidal flows in the Arabian Gulf, in: Computational Techniques and Applications: CTAC-89, Edited by: Hogarth, WL and Noye, BJ, Griffith University, Brisbane, Queensland, Australia, Hemisphere Publishing Corp., New York. pp. 295–302.

Chao, S.-Y., Kao, T.W., Al-Hajri, K.R., 1992. A Numerical Investigation of Circulation in the Arabian Gulf. J. Geophys. Res. 97, 11219–11236. https://doi.org/10.1029/92jc00841

Chu, W. Sen, Barker, B.L., Akbar, A.M., 1988. Modeling tidal transport in the Arabian gulf. J. Waterw. Port, Coast. Ocean Eng. https://doi.org/10.1061/(ASCE)0733-950X(1988)114:4(455)

Egbert, G.D., Bennett, A.F., Foreman, M.G.G., 1994. TOPEX/POSEIDON tides estimated using a global inverse model. J. Geophys. Res. Ocean. 99, 24821–24852.

Egbert, G.D., Erofeeva, S.Y., 2002. Efficient inverse modeling of barotropic ocean tides. J. Atmos. Ocean. Technol. 19, 183–204.

Farmer, D.M., Armi, L., 1986. Maximal two-layer exchange over a sill and through the combination of a sill and contraction with barotropic flow. J. Fluid Mech. https://doi.org/10.1017/S002211208600246X

Foreman, M.G.G., 1978. Manual for Tidal Currents Analysis and Prediction, Pacific Marine Science Report 78-6, Institute of Ocean Sciences, Patricia Bay, Sidney, British Columbia.

Hetzel, Y., Pattiaratchi, C., Lowe, R., Hofmeister, R., 2015. Wind and tidal mixing controls on stratification and dense water outflows in a large hypersaline bay. J. Geophys. Res. Ocean. https://doi.org/10.1002/2015JC010733

Hughes, P., Hunter J.R., 1979. Physical oceangraphy and numerical modeling of the kuwait action plan (KAP) region.

John, V.C., 1992. Harmonic tidal current constituents of the western Arabian Gulf from moored current measurements. Coast. Eng. https://doi.org/10.1016/0378-3839(92)90016-N

Johns, W.E., Yao, F., Olson, D.B., Josey, S.A., Grist, J.P., Smeed, D.A., 2003. Observations of seasonal exchange through the Straits of Hormuz and the inferred heat and freshwater budgets of the Persian Gulf. J. Geophys. Res. Ocean. 108.

Kämpf, J., Sadrinasab, M., 2006. The circulation of the Persian Gulf: a numerical study. Ocean Sci. 2, 27–41.

Khonkar, H., 2009. Complete survey of wind behavior over the Arabian Gulf. J. King Abdulaziz Univ. Mar. Sci. https://doi.org/10.4197/Mar.20-1.3

Kurogi, M., Hasumi, H., 2019. Tidal control of the flow through long, narrow straits: a modeling

study for the Seto Inland Sea. Sci. Rep. https://doi.org/10.1038/s41598-019-47090-y
Lardner, R.W., Al-Rabeh, A.H., Gunay, N., Cekirge, H.M., 1989. Implementation of the three-dimensional hydrodynamic model for the Arabian Gulf. Adv. Water Resour. 12, 2–8. https://doi.org/10.1016/0309-1708(89)90010-9
Lardner, R.W., Belen, M.S., Cekirge, H.M., 1982. Finite difference model for tidal flows in the Arabian Gulf. Comput. Math. with Appl. 8, 425–444. https://doi.org/10.1016/0898-1221(82)90018-9
Lardner, R.W., Cekirge, H.M., 1988. A new algorithm for three-dimensional tidal and storm surge computations. Appl. Math. Model. 12, 471–481.
Lardner, R.W., Cekirge, H.M., Gunay, N., 1986. Numerical solution of the two-dimensional tidal equations using the method of characteristics. Comput. Math. with Appl. 12, 1065–1080.
Large, W.G., Danabasoglu, G., Doney, S.C., Mcwilliams, J.C., 1997. Sensitivity to surface forcing and boundary layer mixing in a global ocean model: Annual-mean climatology. J. Phys. Oceanogr.
Large, W.G., McWilliams, J.C., Doney, S.C., 1994. Oceanic vertical mixing: A review and a model with a nonlocal boundary layer parameterization. Rev. Geophys. 32, 363–403.
Marshall, J., Adcroft, A., Hill, C., Perelman, L., Heisey, C., 1997. A finite-volume, incompressible Navier Stokes model for studies of the ocean on parallel computers. J. Geophys. Res. Ocean. 102, 5753–5766. https://doi.org/10.1029/96JC02775
Mashayekh Poul, H., Backhaus, J., Dehghani, A., Huebner, U., 2016a. Effect of subseabed salt domes on Tidal Residual currents in the Persian Gulf. J. Geophys. Res. Ocean. 121, 3372–3380.
Mashayekh Poul, H., Backhaus, J., Huebner, U., 2016b. A description of the tides and effect of Qeshm canal on that in the Persian Gulf using two-dimensional numerical model. Arab. J. Geosci. https://doi.org/10.1007/s12517-015-2259-8
Naranjo, C., Garcia-Lafuente, J., Sannino, G., Sanchez-Garrido, J.C., 2014. How much do tides affect the circulation of the Mediterranean Sea? From local processes in the Strait of Gibraltar to basin-scale effects. Prog. Oceanogr. https://doi.org/10.1016/j.pocean.2014.06.005
Nayak, R.K., Salim, M., Mitra, D., Sridhar, P.N., Mohanty, P.C., Dadhwal, V.K., 2015. Tidal and Residual Circulation in the Gulf of Khambhat and its Surrounding on the West Coast of India. J. Indian Soc. Remote Sens. 43, 151–162.
Pous, S., Carton, X., Lazure, P., 2012. A Process Study of the Tidal Circulation in the Persian Gulf. Open J. Mar. Sci. https://doi.org/10.4236/ojms.2012.24016
Pous, S., Lazure, P., Carton, X., 2015. A model of the general circulation in the Persian Gulf and in the Strait of Hormuz: Intraseasonal to interannual variability. Cont. Shelf Res. 94, 55–70. https://doi.org/10.1016/j.csr.2014.12.008
Proctor, R., Elliott, A.J., Flather, R.A., 1992. Predictions and observations of the Arabian Gulf oil slick. J. Nitride Semicond. 17, 215–227.
Reynolds, R.M., 1993. Physical oceanography of the Gulf, Strait of Hormuz, and the Gulf of Oman—Results from the Mt Mitchell expedition. Mar. Pollut. Bull. 27, 35–59.
Rocha, C.B., Chereskin, T.K., Gille, S.T., Menemenlis, D., 2016. Mesoscale to submesoscale wavenumber spectra in Drake Passage. J. Phys. Oceanogr. 46, 601–620.
Sabbagh-Yazdi, S.R., Zounemat-Kermani, M., Kermani, A., 2007. Solution of depth-averaged tidal currents in Persian Gulf on unstructured overlapping finite volumes. Int. J. Numer. Methods Fluids. https://doi.org/10.1002/fld.1441
Sannino, G., Bargagli, A., Artale, V., 2004. Numerical modeling of the semidiurnal tidal exchange

through the Strait of Gibraltar. J. Geophys. Res. C Ocean. https://doi.org/10.1029/2003JC002057
Sannino, G., Carillo, A., Pisacane, G., Naranjo, C., 2015. On the relevance of tidal forcing in modelling the Mediterranean thermohaline circulation. Prog. Oceanogr. 134, 304–329. https://doi.org/10.1016/j.pocean.2015.03.002
Smith, W.H.F., Sandwell, D.T., 1997. Global sea floor topography from satellite altimetry and ship depth soundings. Science (80-.). 277, 1956–1962.
Swift, S.A., Bower, A.S., 2003. Formation and circulation of dense water in the Persian/Arabian Gulf. J. Geophys. Res. Ocean. 108.
Thoppil, P.G., Hogan, P.J., 2010a. Persian Gulf response to a wintertime shamal wind event. Deep. Res. Part I Oceanogr. Res. Pap. 57, 946–955. https://doi.org/10.1016/j.dsr.2010.03.002
Thoppil, P.G., Hogan, P.J., 2010b. A Modeling Study of Circulation and Eddies in the Persian Gulf. J. Phys. Oceanogr. 40, 2122–2134.
Vasou, P., Vervatis, V., Krokos, G., Hoteit, I., Sofianos, S., 2020. Variability of water exchanges through the Strait of Hormuz. Ocean Dyn. 70, 1053–1065.
Von Trepka, L., 1968. Investigation of the tides in the Persian Gulf by means of a hydrodynamic numerical model, in: Proceeding of Symposium on Mathematical Hydrological Investigations of Physical Process in the Sea, Inst. pp. 59–63.
Wang, X., Peng, S., Liu, Z., Huang, R.X., Qian, Y.-K., Li, Y., 2015. Tidal Mixing in the South China Sea: An Estimate Based on the Internal Tide Energetics. J. Phys. Oceanogr. 46, 107–124. https://doi.org/10.1175/jpo-d-15-0082.1
Warner, J.C., Sherwood, C.R., Arango, H.G., Signell, R.P., 2005. Performance of four turbulence closure models implemented using a generic length scale method. Ocean Model. 8, 81–113. https://doi.org/10.1016/j.ocemod.2003.12.003
Willmott, C.J., 1981. On the validation of models. Phys. Geogr. https://doi.org/10.1080/02723646.1981.10642213

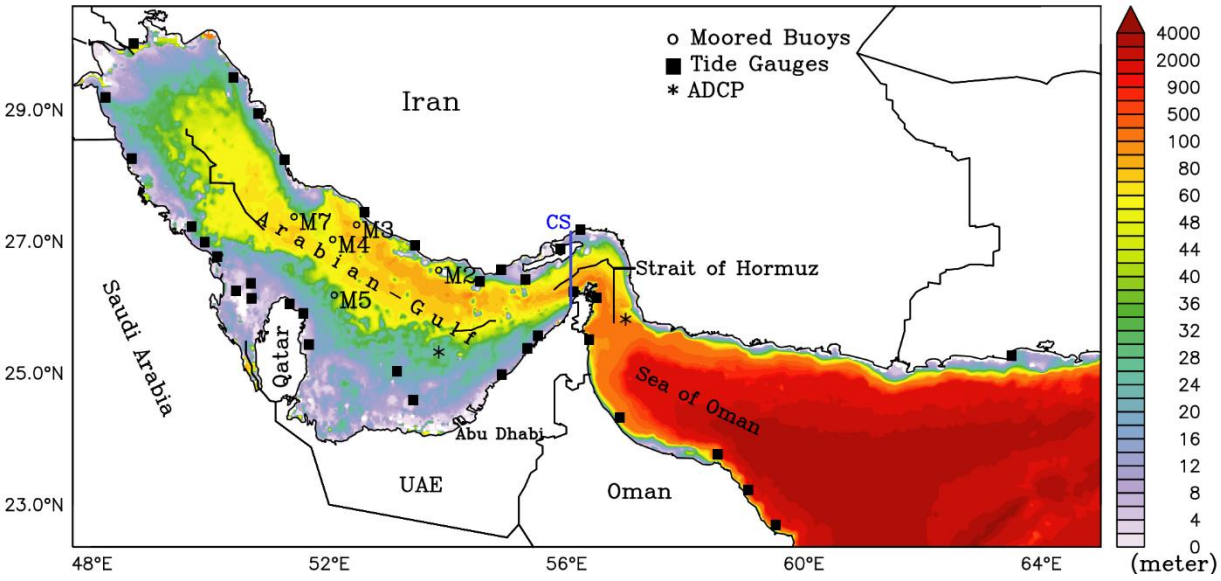

Figure 1. Study area and bathymetry (color scale in meters) with marked locations of (i) tide guage/sea level measurements (black boxes) (ii) mooring locations M2, M3, M4, M5 and M7 (o) and (iii) ADCPs represented by (*). CS is the cross section at which the inflow, outflow and exchange is calculated in the proximity of the Strait of Hormuz.

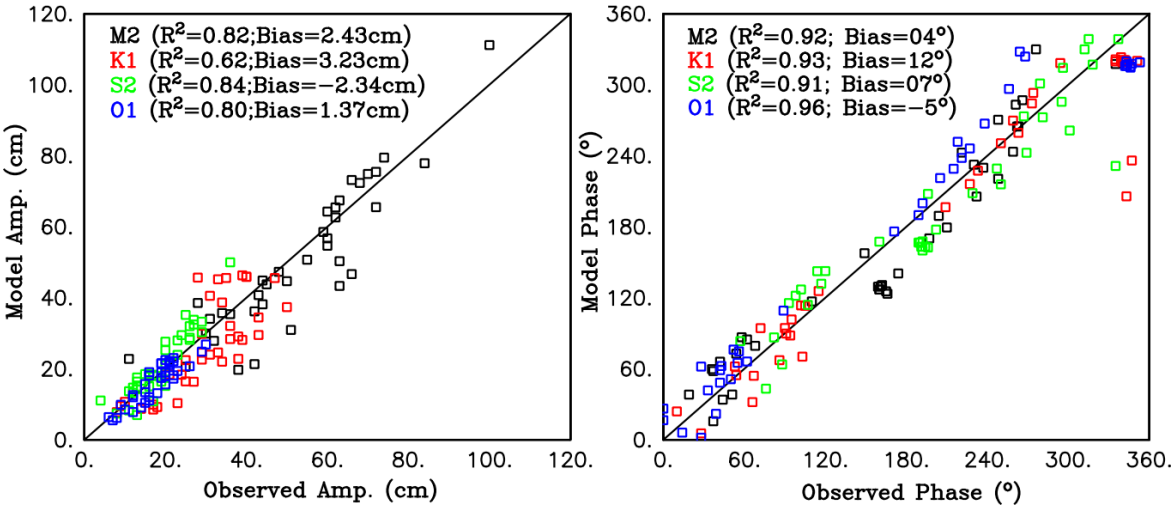

Figure 2. Observed vs model amplitude and phases of major tidal constituents (M2, S2, K1, O1) at the position of tide guages: color coding is black, red, green and blue squares for the M2, K1, S2 and O1 tidal consituents respectively. The model run is carried out with only tidal forcing at the open boundary.

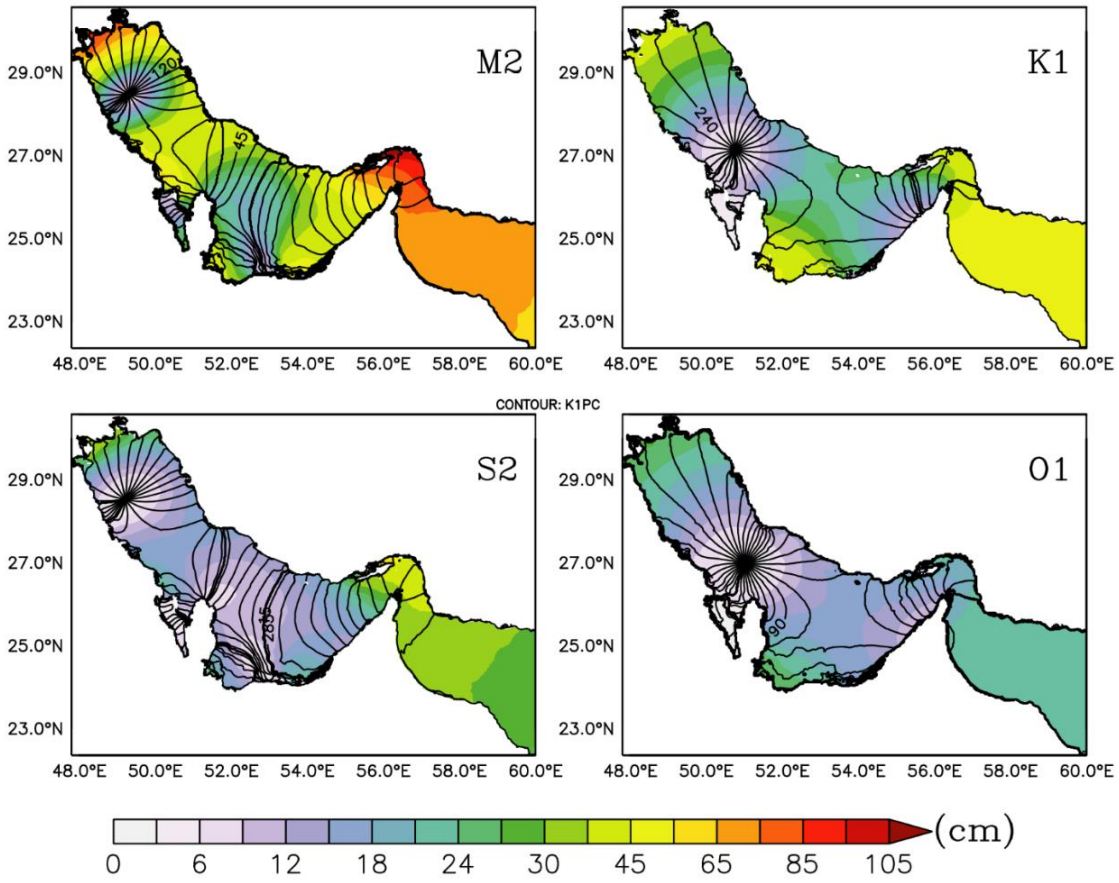

Figure 3. Model derived amplitudes in cm (shaded in colors) overlaid with phase contours of the major tidal constituents (M2, S2, K1 and O1). The model run is carried out with only tidal forcing at the open boundary.

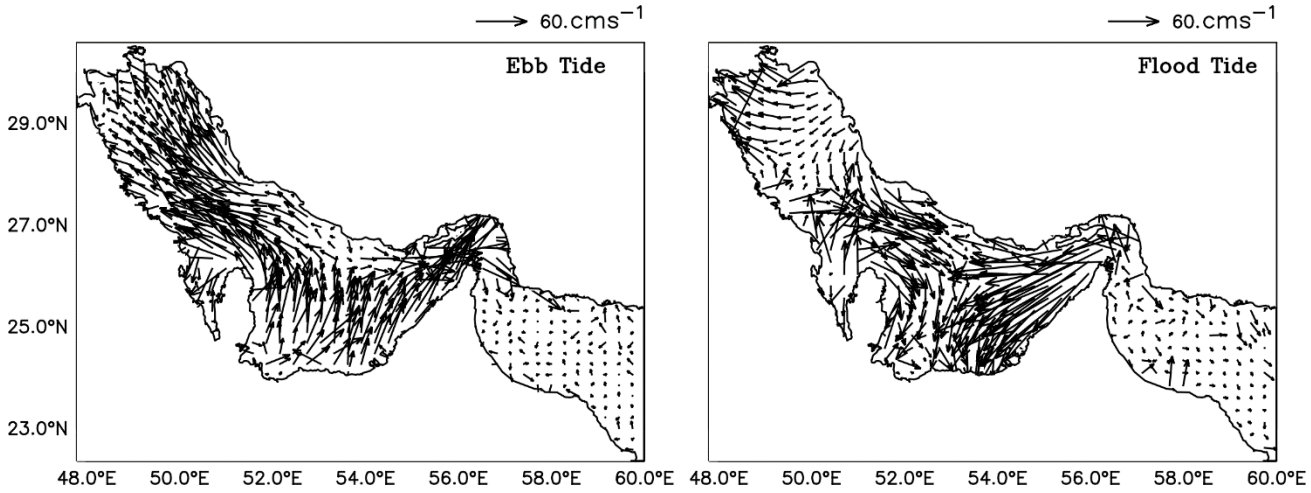

Figure 4. The vector plots of surface currents during Ebb and Flood tide phases in the Gulf. The ebb and flood are the current at a time when the tidal level is at a peak and minimum respectively. The model simulations are carried out with only tidal forcing at the open boundary.

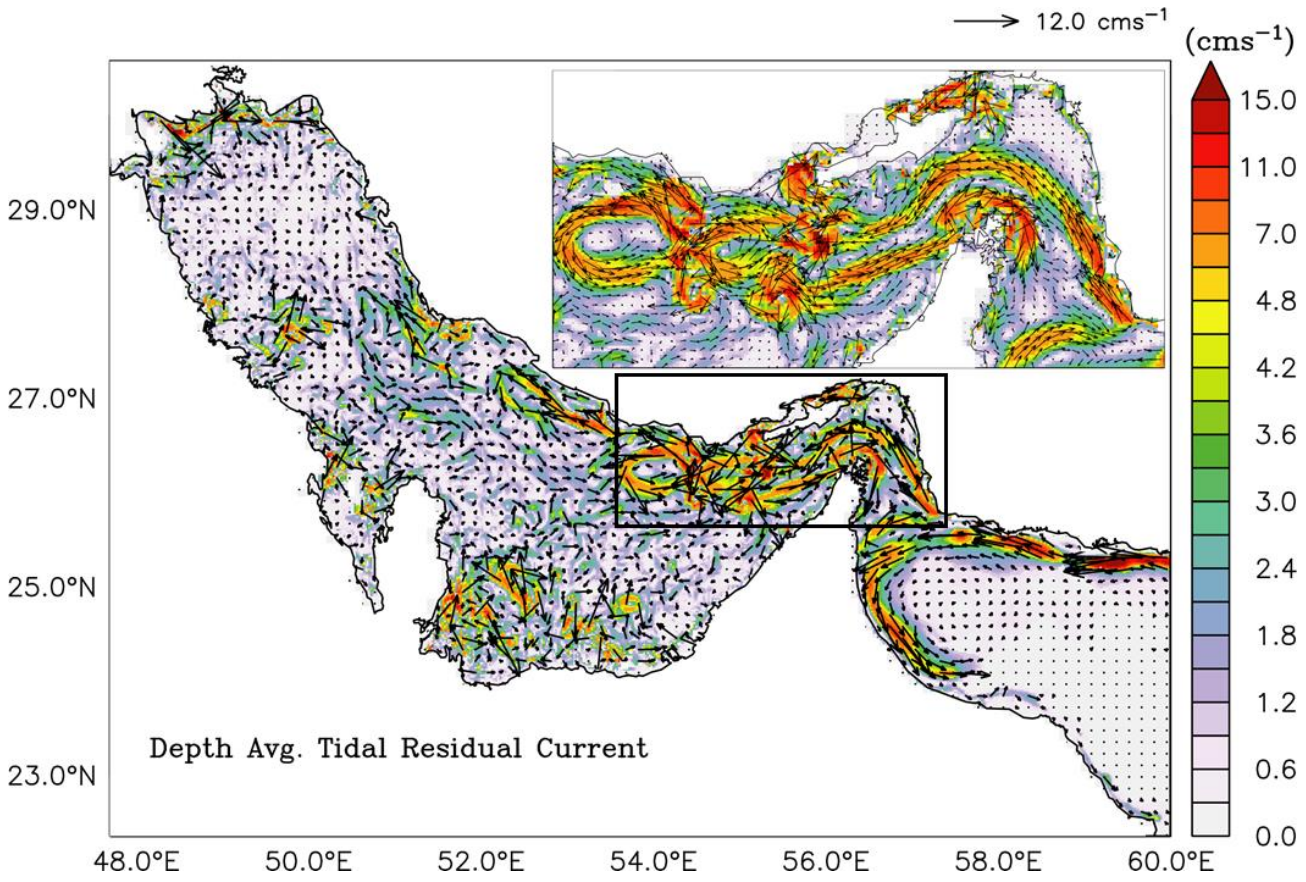

Figure 5. The depth-averaged tide-induced residual currents (in cms^{-1}) extracted from the tide only run averaged over multiple tidal cycles. The zoomed image of the Strait of Hormuz is shown in the inset on the top right. The speeds range from low in grey to high in red.

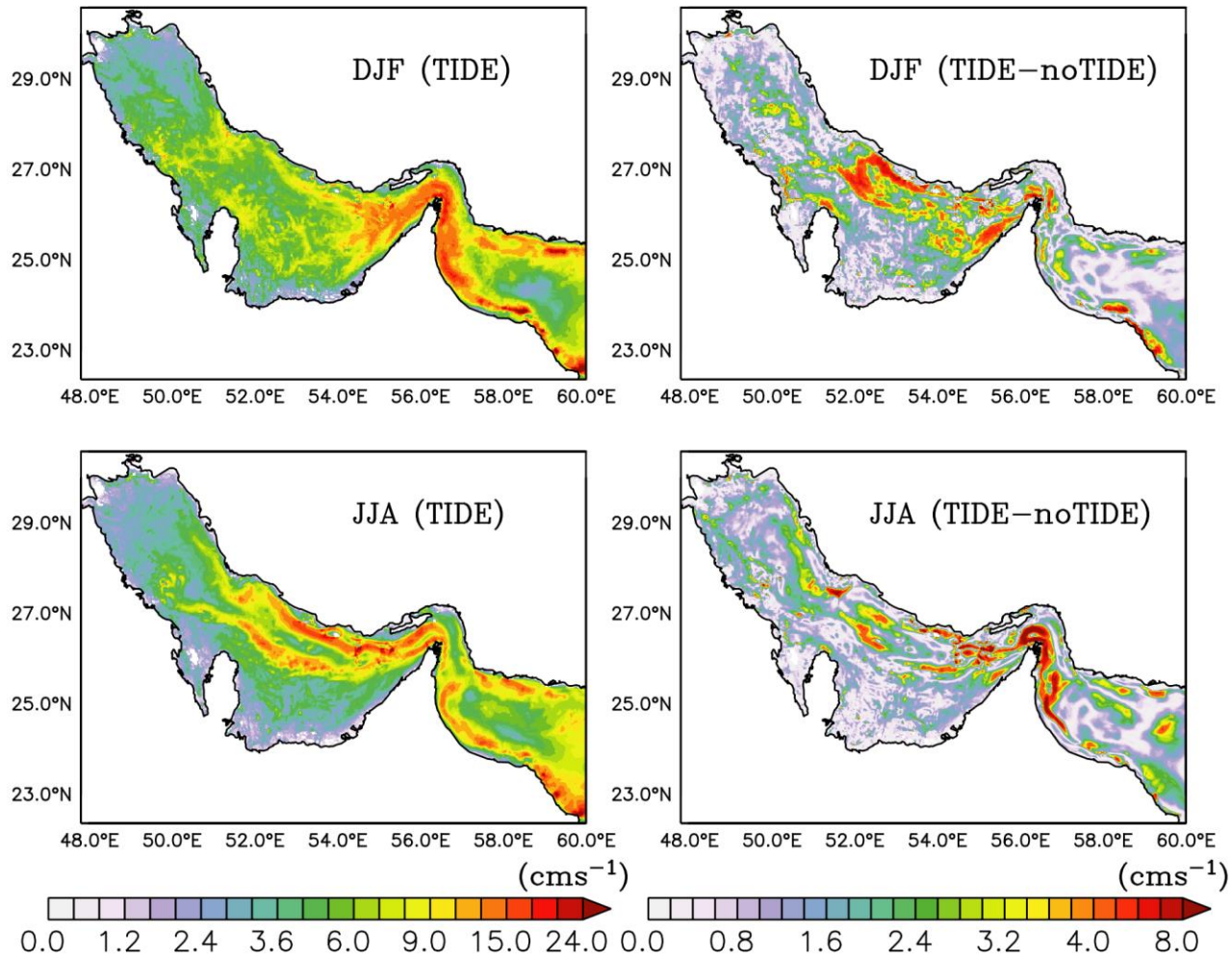

Figure 6. Upper and lower left panels show the depth-averaged current speed during summer and winter driven by all forcing plus tides. The upper and lower right panel shows the absolute difference between the speeds of model runs with all forcing plus tides and all forcing except tides at the open boundary.

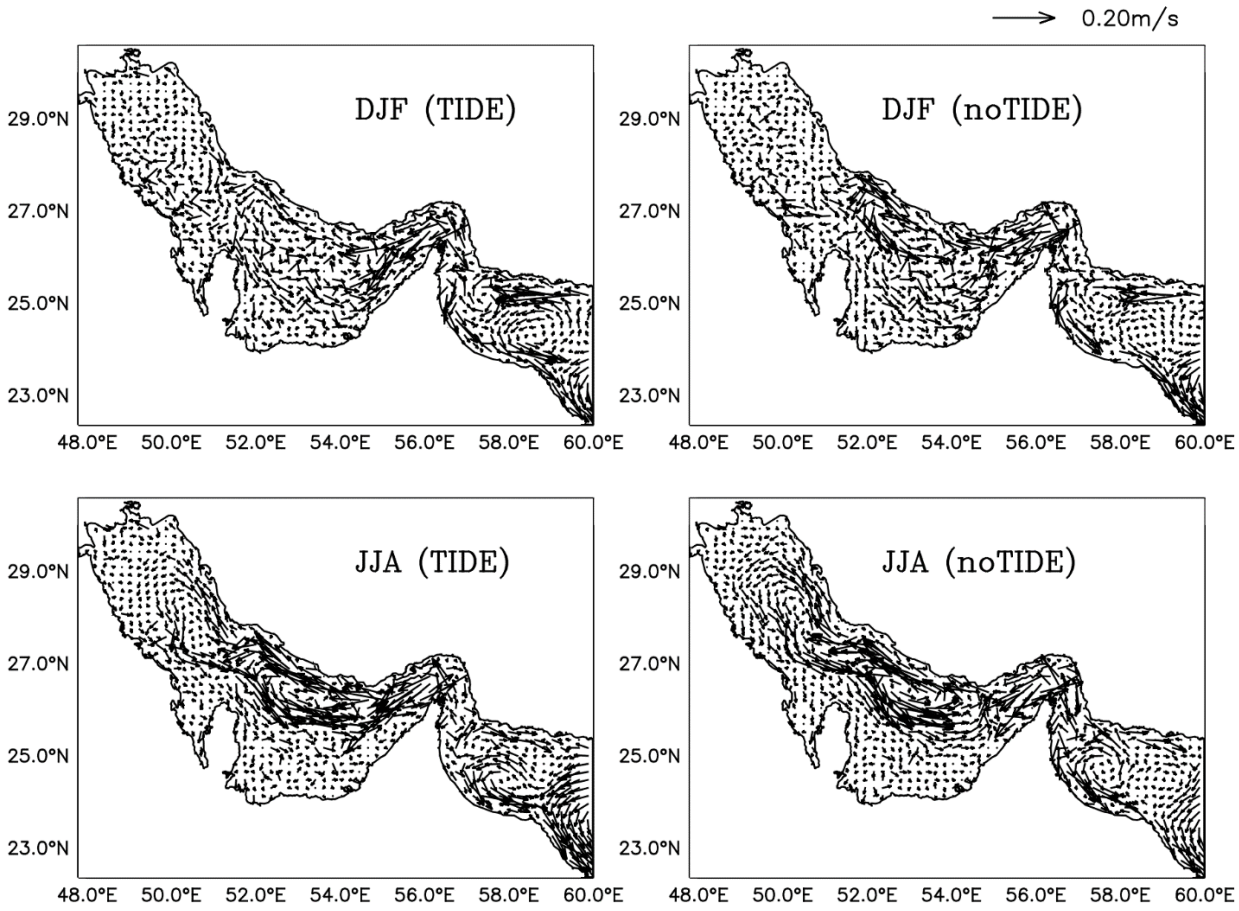

Figure 7. The upper left and lower left panels show the depth-averaged current vectors in ms^{-1}, of the model run with all forcing plus tides during winter and summer. The upper right and lower right panel show model current vectors with all forcing except tides at the open boundary.

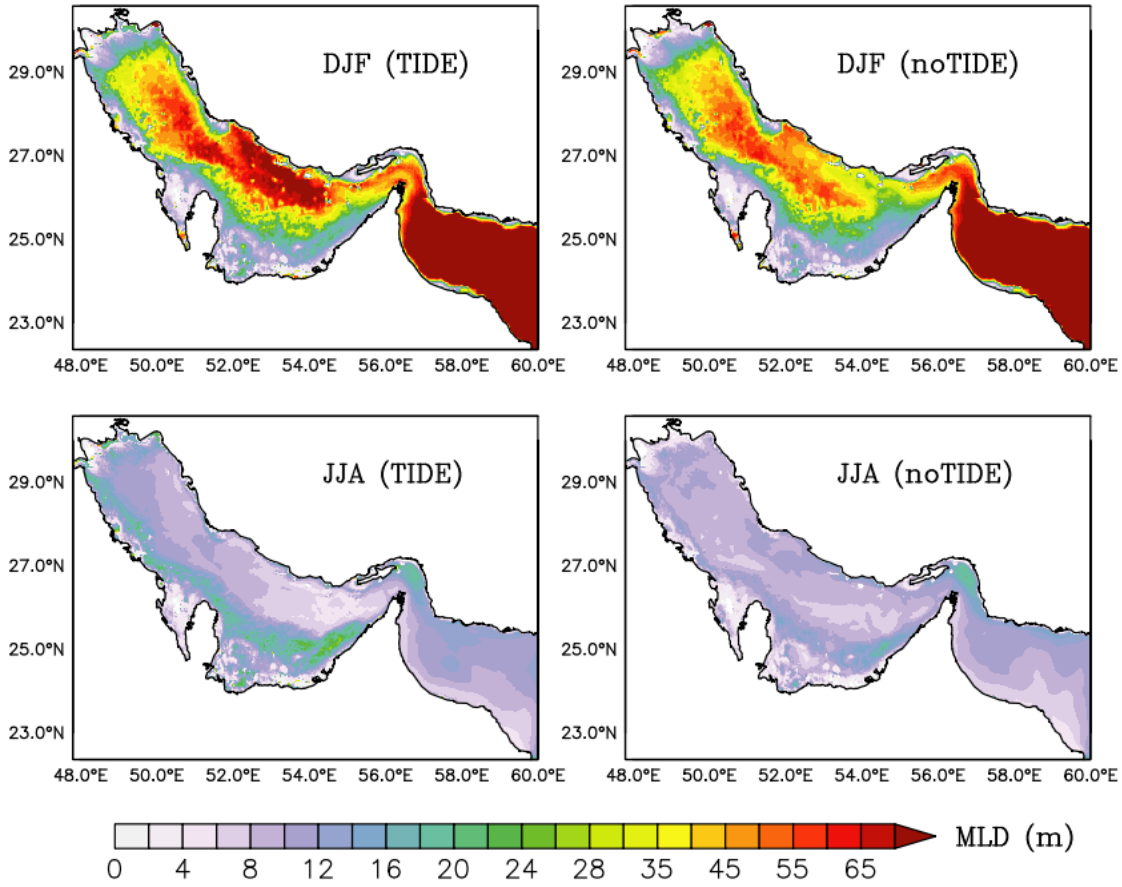

Figure 8. The model simulated mixed layer depth (MLD) maps (in meters) with 'all forcing' plus tides (left panels) and 'all forcing' without tides (right panels) during winter (DJF) and summer (JJA).

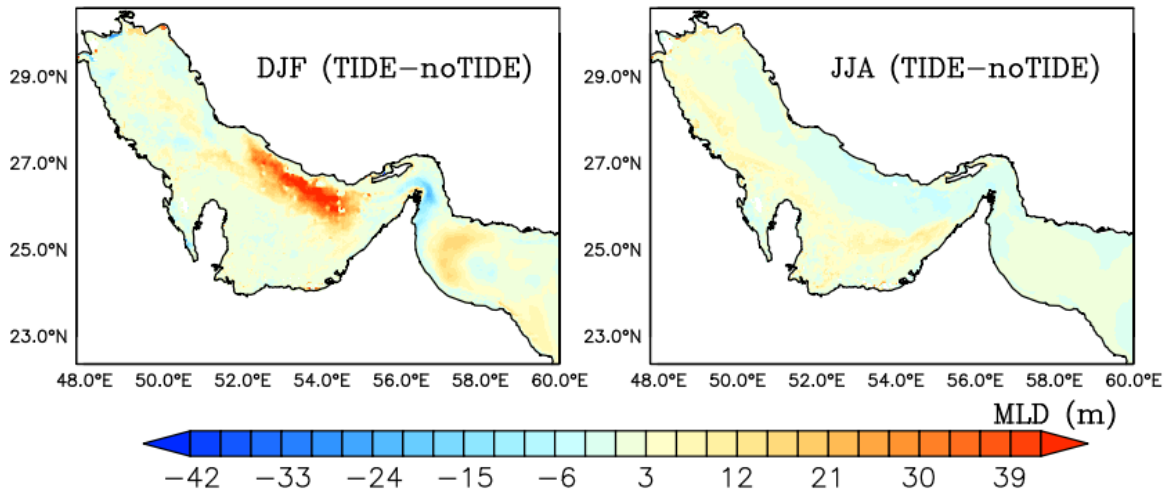

Figure 9. The difference maps of simulated mixed layer depth (MLD) between the simulations of all forcing with tides and without tides at the Gulf in meters during winter (DJF) and summer (JJA).

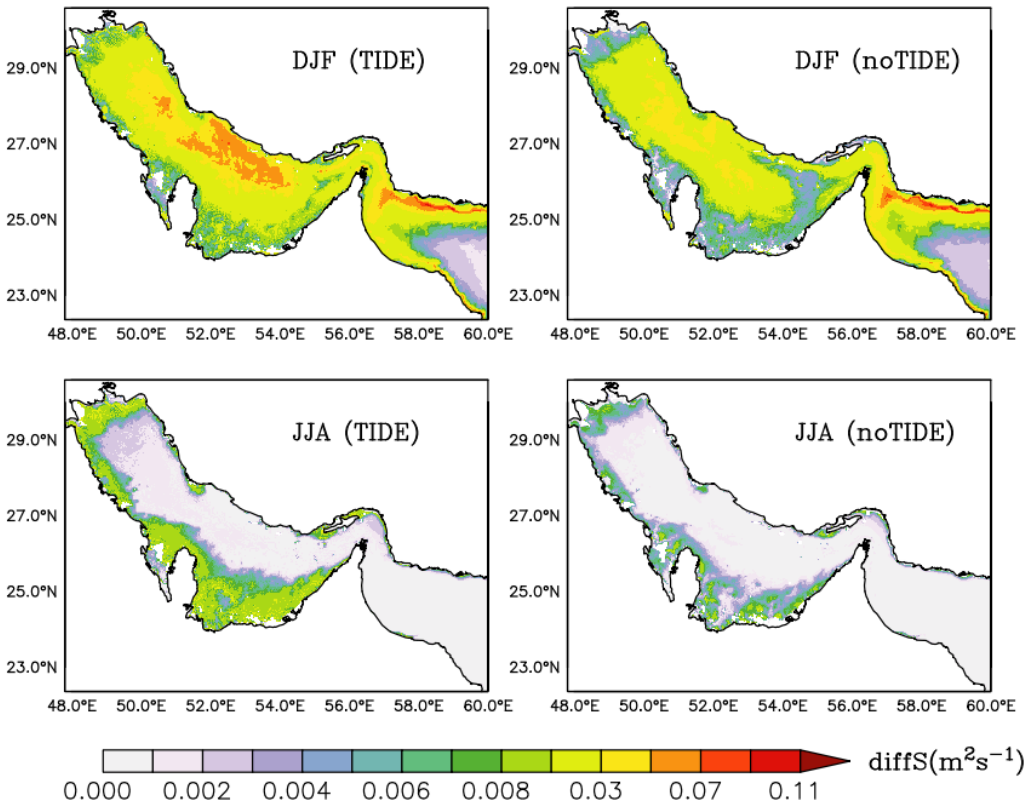

Figure 10. Simulated depth-averaged diffusivity maps with 'all forcing' plus tides (left panels) and 'all forcing' without tides (right panels) during winter (DJF) and summer (JJA) in m^2s^{-1}.

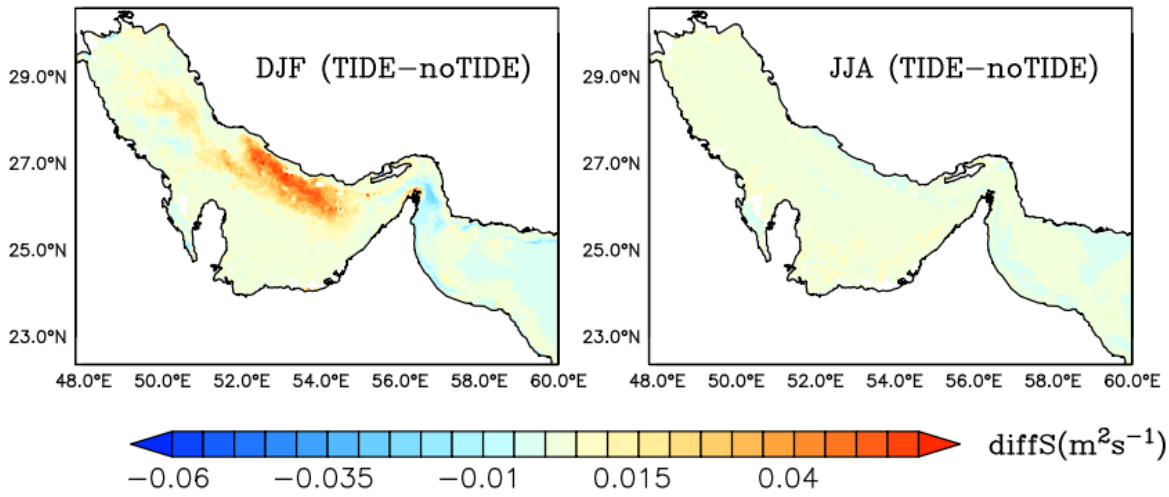

Figure 11. The difference maps of depth-averaged diffusivity between the simulations of 'all forcing' with tides and without tides during winter (DJF) and summer (JJA) in m^2s^{-1}.

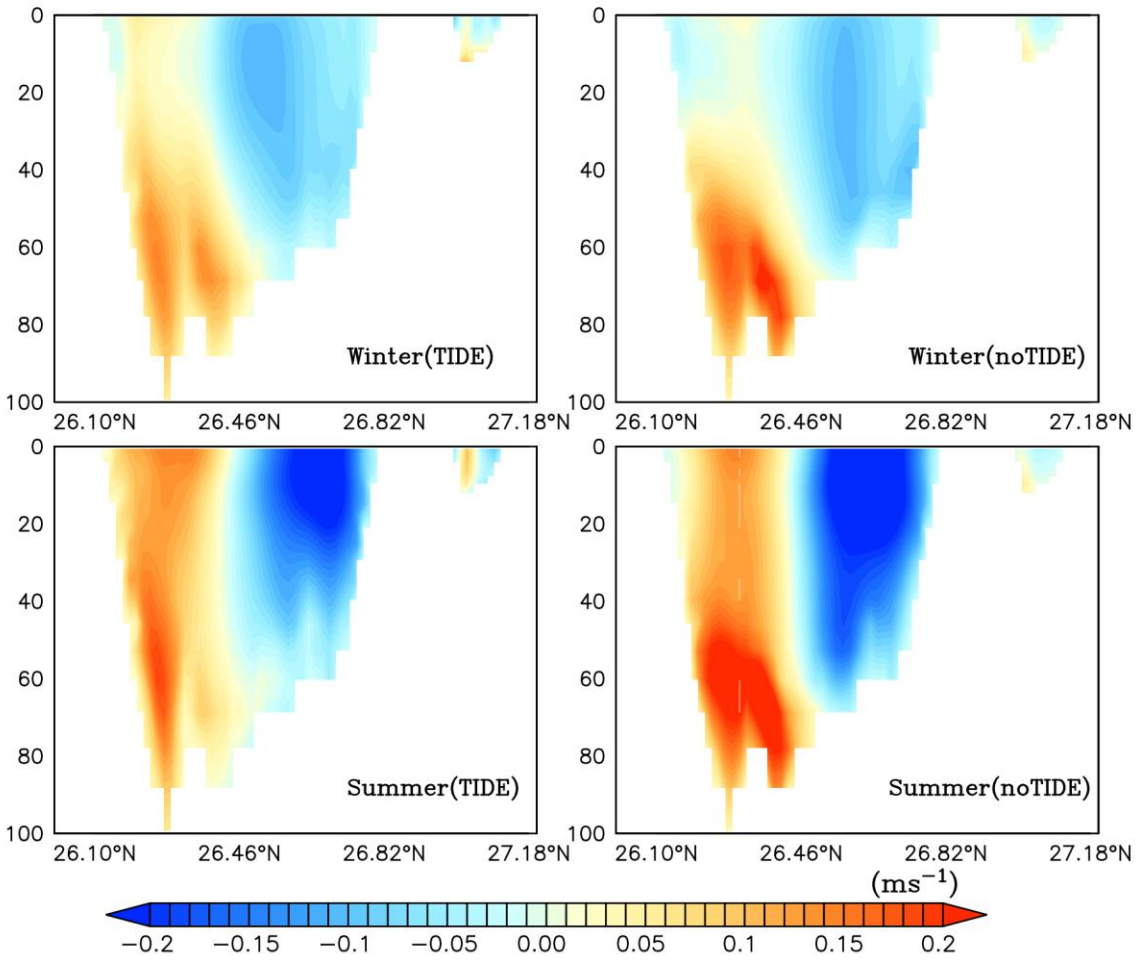

Figure 12. A vertical cross section (along CS see Figure1) of the flow directed through the Strait of Hormuz. The positive values show outflow (red) and the negative values (blue) show inflow. Left panels are obtained with 'all forcing' plus tides on the open boundary and the right panels correspond to 'all forcing' without tidal forcing.

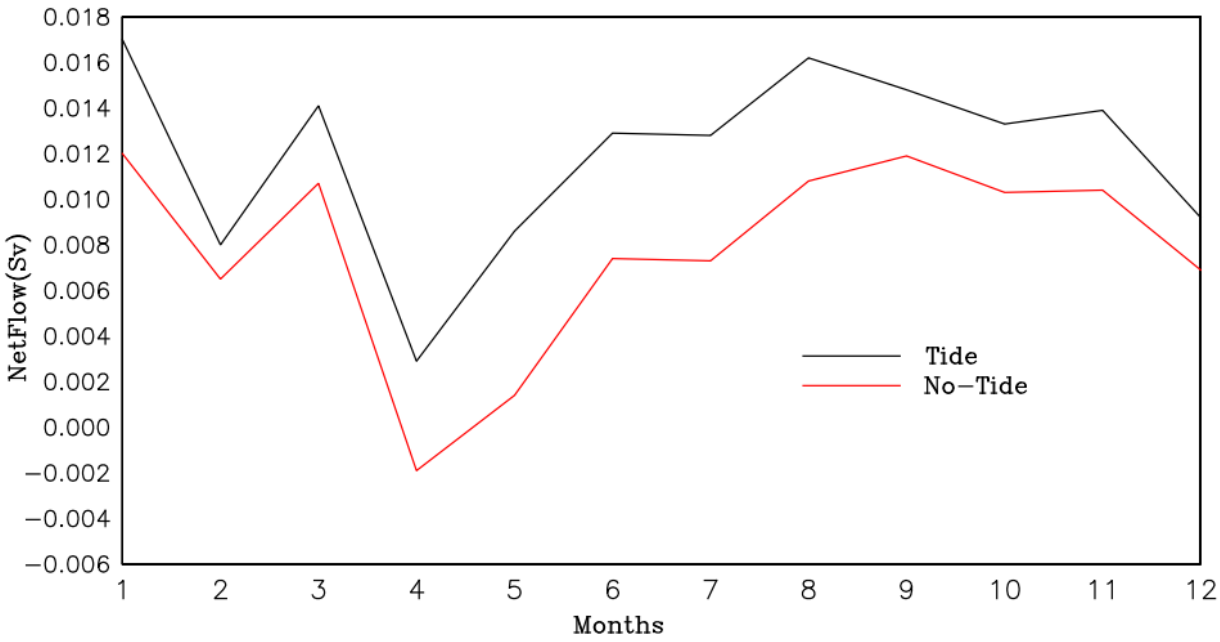

Figure 13. Net flows in Sverdrups through CS at the Strait of Hormuz. A positive sign indicates inflow and negative outflow. The black solid line is from an all forcing run with tides on the open boundary and the red line from an all forcing run without tidal forcing.

APPENDIX

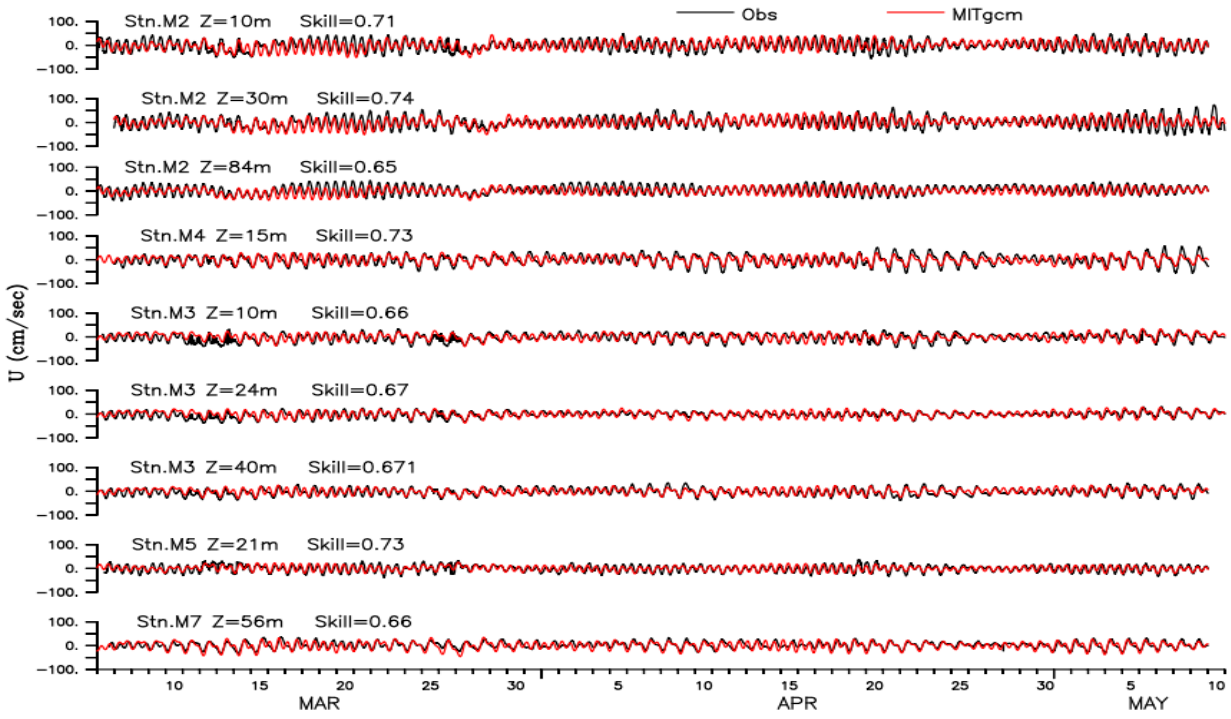

Figure A1. Comparison of modeled and observed zonal currents at chosen mooring locations and depths.

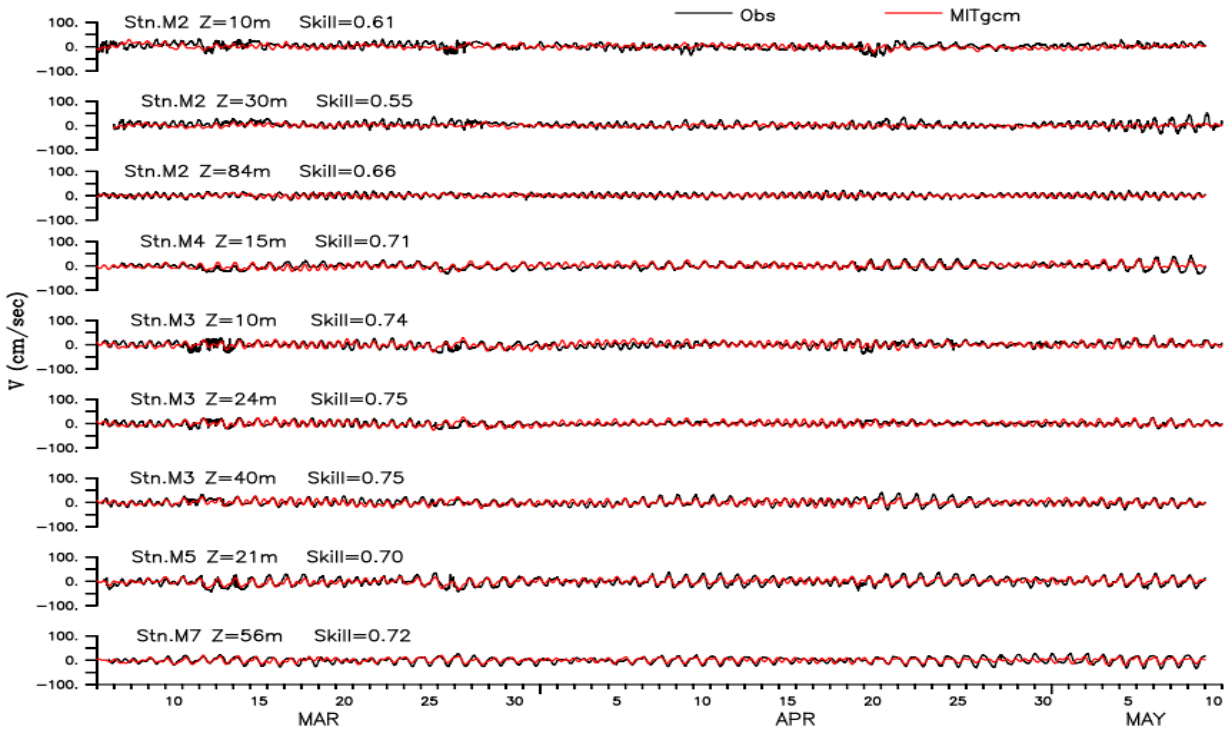

Figure A2. Comparison of modeled and observed meridional currents at chosen mooring locations and depths.